



Published in final edited form as:

Neuroscience. 2007 March 30; 145(3): 1037–1047.

Environmental Pb²⁺ exposure during early life alters granule cell neurogenesis and morphology in the hippocampus of young adult rats

Tatyana Verina¹, Charles A. Rohde², and Tomás R. Guilarte^{1,*}

1 Neurotoxicology & Molecular Imaging Laboratory, Johns Hopkins University Bloomberg School of Public Health, Baltimore, Maryland. 21205

2 Department of Environmental Health Sciences & Department of Biostatistics, Johns Hopkins University Bloomberg School of Public Health, Baltimore, Maryland. 21205

Abstract

Exposure to environmentally relevant levels of lead (Pb²⁺) during early life produces deficits in hippocampal synaptic plasticity in the form of long-term potentiation (LTP) and spatial learning in young adult rats (Nihei et al., 2000; Guilarte et al., 2003). Other evidence suggests that the performance of rats in the Morris water maze spatial learning tasks is associated with the level of granule cell neurogenesis in the dentate gyrus (DG) (Drapeau et al., 2003). In this study, we examined whether continuous exposure to environmentally relevant levels of Pb²⁺ during early life altered granule cell neurogenesis and morphology in the rat hippocampus. Control and Pb²⁺-exposed rats received BrdU injections (100 mg/kg; i.p.) for five consecutive days starting at postnatal day 45 and were sacrificed either one day or four weeks after the last injection. The total number of newborn cells in the DG of Pb²⁺-exposed rats was significantly decreased (13%; p<0.001) one day after BrdU injections relative to controls. Further, the survival of newborn cells in Pb²⁺-exposed rats was significantly decreased by 22.7% (p<0.001) relative to control animals. Co-localization of BrdU with neuronal or astrocytic markers did not reveal a significant effect of Pb²⁺ exposure on cellular fate. In Pb²⁺-exposed rats, immature granule cells immunolabeled with doublecortin (DCX) displayed aberrant dendritic morphology. That is, the overall length-density of the DCX-positive apical dendrites in the outer portion of the DG molecular layer was significantly reduced up to 36% in the suprapyramidal blade only. We also found that the area of Timm's-positive staining representative of the mossy fibers terminal fields in the CA3 stratum oriens (SO) was reduced by 26% in Pb²⁺-exposed rats. These findings demonstrate that exposure to environmentally relevant levels of Pb²⁺ during early life alter granule cell neurogenesis and morphology in the rat hippocampus. They provide a cellular and morphological basis for the deficits in synaptic plasticity and spatial learning documented in Pb²⁺-exposed animals.

Keywords

Neurogenesis; granule cell; mossy fibers; dendrites; morphology; hippocampus; lead (Pb²⁺); rat brain; neurotoxicity

*Corresponding author: Tomás R. Guilarte, PhD, Department of Environmental Health Sciences, Johns Hopkins Bloomberg School of Public Health 615 North Wolfe St, Room E6622, Baltimore, Maryland. 21205, Phone: (410) 955-2485, Fax: (410) 502-2470, E-mail: tguilart@jhsph.edu

Publisher's Disclaimer: This is a PDF file of an unedited manuscript that has been accepted for publication. As a service to our customers we are providing this early version of the manuscript. The manuscript will undergo copyediting, typesetting, and review of the resulting proof before it is published in its final citable form. Please note that during the production process errors may be discovered which could affect the content, and all legal disclaimers that apply to the journal pertain.

Introduction

Human exposure to environmental levels of lead (Pb^{2+}) is a public health problem of global proportion. Pb^{2+} is a pervasive environmental pollutant and chronic exposure to this neurotoxicant impairs synaptic plasticity in the form of long-term potentiation (LTP) and cognitive function in experimental animals (see review by Toscano and Guilarte, 2005). The detrimental effects of Pb^{2+} on LTP and spatial learning have been attributed to the fact that Pb^{2+} is a selective and potent inhibitor of the *N*-methyl-*D*-aspartate subtype of excitatory amino acid receptors (NMDAR) (Alkondon et al., 1990; Guilarte and Miceli, 1992; Gavazzo et al., 2001). Further, chronic exposure to Pb^{2+} during early life alters the expression of NMDAR subunits in the rat hippocampus (Guilarte and McGlothan, 1998; Nihei and Guilarte 1999; Guilarte et al., 2000; Nihei et al., 2000) affecting NMDAR complex composition (Toscano et al., 2002) and downstream calcium signaling (Toscano et al., 2003). Therefore, there is compelling experimental evidence that chronic Pb^{2+} exposure alters NMDAR function in the rat hippocampus and this effect is associated with impairments in hippocampal LTP and spatial learning in young adult rats (Nihei et al., 2000; Toscano and Guilarte, 2005).

NMDAR are abundantly expressed in the hippocampus and play an important role in regulating neuronal development, synaptic plasticity and learning and memory (Lynch, 2004; Nakazawa et al., 2004). Experimental evidence also suggests that modulation of excitatory amino acid neurotransmission and NMDAR activity alters granule cell neurogenesis in the rat hippocampus (Abrous et al., 2005; Nacher and McEwen, 2006). Removal of excitatory input to the granule cell layer (GCL) from the entorhinal cortex by excision of the perforant path or acute pharmacological NMDAR inhibition increases granule cell neurogenesis (Gould, 1994; Cameron et al., 1995; Gould et al., 1997; Cameron et al., 1998; Nacher et al., 2003). On the other hand, other studies have noted that direct excitatory stimulation of adult hippocampal progenitor stem cells from rodents (Deisseroth et al., 2004) or humans (Suzuki et al., 2006) favors neurogenesis by direct activation of NMDAR and L-type calcium channels. Conversely, inhibition of NMDAR decreases neurogenesis (Deisseroth et al., 2004). Also, under pathological conditions such as in seizures and stroke, inhibition of NMDAR function decreases granule cell neurogenesis (Parent et al., 1997; Barnbeau and Sharp, 2000; Arvidsson et al., 2001). Chun et al., (2006) have recently demonstrated that tetanic stimulation of perforant path-DG synapses that induces LTP results in an increase in granule cell neurogenesis suggesting that NMDAR-dependent activity is positively linked to DG neurogenesis. Lastly, cell-specific deletion of the NR1 subunit of the NMDAR in newly born neurons of the DG reduces their survival, an effect attributable to their inability to sense surrounding synaptic activity via NMDAR activation (Tashiro et al., 2006). Taken together these studies indicate that NMDAR activity is coupled to granule cell neurogenesis in the hippocampus, but the mechanisms are complex and not fully understood (Nacher and McEwen, 2006).

In the present study, we tested the hypothesis that chronic exposure to environmentally relevant levels of Pb^{2+} during early life alters granule cell neurogenesis in the hippocampus of young adult rats. Since newly born granule cells mature and become incorporated into the dentate gyrus-CA3 circuitry, we also examined the morphology of their apical dendrites and their mossy fiber connections to the CA3 region. The studies were performed using a chronic Pb^{2+} exposure paradigm documented to produce deficits in perforant path-DG-LTP and impairments of spatial learning in young adult rats (Nihei et al., 2000; Guilarte et al., 2003).

Materials and Methods

Animal husbandry and Pb^{2+} analysis

Female Long-Evans rats (225–250 g) were purchased from Charles River, Inc. (Wilmington, MA) and fed 0 or 1500-ppm Pb^{2+} acetate. The Pb^{2+} acetate was incorporated into the rat chow

mix (RMH 1000) and the food mixture was made into pellets by the manufacturer (Dyets, Bethlehem, PA). Feeding of the Pb²⁺-containing and control diets was initiated 10 days before breeding females to untreated Long-Evans male rats. Dams were maintained on their respective diets during gestation and lactation. Litters were culled to 10 animals (maintaining the maximal number of male rats) one day after birth and weaned at postnatal day (PN) 21 at which time they were fed the same diet as their corresponding mother (Figure 1). Litters of rats were considered one experimental unit for statistical purposes. Therefore, for each experiment one animal was used per litter to generate a single data point. Multiple litters were used for any one measurement. All animal studies were reviewed and approved by the Johns Hopkins University Animal Care and Use Committee. Rat diet was analyzed for Pb²⁺ content by an independent laboratory (ESA Laboratories, Inc. Chelmsford, MA) to verify that it contained the appropriate Pb²⁺ concentration. Blood Pb²⁺ levels were analyzed using Lead Care-Blood Testing System as described by manufacturer's instructions (ESA Laboratories, Inc. Chelmsford, MA).

BrdU administration

To label newly born cells we used the thymidine analog bromodeoxyuridine (BrdU) incorporation into DNA during the S-phase of the cell cycle (Nowakowski, 1989). All groups of animal received intraperitoneal injections of BrdU (Roche, Indianapolis, IN) once a day (100 mg/kg body weight) for five consecutive days starting at PN45 (Figure 1). For the proliferation study, rats (controls n=7, Pb²⁺-treated n=9) were sacrificed one day after the last BrdU injection at PN50. For the survival study, a second group of rats (controls n=6, Pb²⁺-treated n=5) was sacrificed four weeks after the last BrdU injection at PN78. BrdU injections were administered at the same time of the morning cycle.

Brain tissue preparation

Rats were perfused transcardially with 100 ml phosphate-buffered saline followed by 450 ml of 4% paraformaldehyde in 0.1M phosphate buffer (PB). After perfusion, brains were removed, post-fixed overnight in the same fixative, cryoprotected with 30% sucrose, and cut in the coronal plane through the dorsal hippocampus into 40 µm thick sections using a freezing microtome (Leica SM2000R).

Antibodies

We used primary antibodies against BrdU (mouse IgG, Roche, 1:400; rat IgG Accurate, 1:100), doublecortin (DCX, goat IgG, Santa Cruz, 1:2000), GFAP (rabbit IgG, DAKO, 1:1000). Corresponding biotinylated secondary antibodies (1:200) and avidin-biotin-peroxidase complex (1:50) solution were purchased from Vector Laboratories (Burlingame, CA). Corresponding fluorophore-conjugated antibodies (Texas Red-donkey-anti-mouse, FITC-donkey-anti-goat, Cy5-donkey-anti-rabbit (1:200) were purchased from Jackson Immunoresearch Laboratories.

Immunohistochemistry and immunofluorescence

To visualize BrdU-positive cells, free-floating sections were first pre-treated to denature DNA. Sections were incubated in 50% formamide in 2x SSC for two hours at 65 C, rinsed with 2x SSC for 15 min, treated with 2N HCl for 30 min at 37 C, rinsed with 0.1M borate buffer (pH 8.5), followed by Tris-buffered saline (TBS). Sections were further pre-treated with 0.6% H₂O₂ for 20 min, rinsed excessively in TBS, pre-treated with 0.2% Triton X-100 for 30 min, blocked in 5% normal serum solution for one hour and incubated with primary antibodies for 24–64 hrs at 4 C. After rinsing in TBS, sections were incubated with corresponding biotinylated secondary IgG (1hr, at room temperature) followed by incubation in the avidin-biotin-peroxidase complex solution (1:50, 30 min at room temperature). The reaction product was visualized using 0.25 mg/ml 3,3'-diaminobenzidine (DAB), 0.03% H₂O₂ with or without

0.04% NiCl₂. Sections were mounted on slides, dehydrated and, when necessary, stained with 0.5% cresyl violet (Chroma-Gesellschaft, Germany). Slides were coverslipped using DPX media (Fluka). For combined immunofluorescence, sections were incubated in a cocktail of primary antibodies followed by incubation in corresponding fluorophore-conjugated secondary antibodies (overnight, at 4 C). Sections were mounted on slides and coverslipped using Pro-long antifade kit (Molecular probes).

BrdU-labeled cell counting

Series of systematically selected brain sections (240 μm apart or every six section) within the extent of the dorsal hippocampus (bregma 7minus;2.8 mm to -4.5 mm) were selected for counting of BrdU-positive cells in both control and Pb²⁺-exposed rats. All slides were coded and the experimenter was blinded prior to microscopic examination. The boundaries of the GCL of the DG and the subgranular zone (SGZ) were defined by Nissl staining and digitally outlined using a x10 objective lens. All BrdU-positive cells within the outlined areas were counted using x100 oil immersion lens. BrdU-labeled cells in the hilus were not counted. We applied identical counting procedures for both the cell proliferation and the cell survival study, but used two different stereological systems due to availability: Stereoinvestigator (MicroBrightField, VT) for the analysis of cell proliferation and CAST (Olympus, Denmark) for the cell survival study. Cell numbers and the corresponding reference area measurements were obtained bilaterally from both the suprapyramidal (SPB) and infrapyramidal (IPB) blades of the DG.

Phenotypic characterization of newly generated cells

Combined immunofluorescence with BrdU as a newborn cell marker, DCX as an immature neuronal marker and GFAP as an astrocytic marker was examined using confocal microscopy (Ultraview, Perkin-Elmer) with a 40x oil objective within the anatomically corresponding fields of the DG in four animals per each treatment group. Z-stacks of 2 μm optical sections were acquired throughout the brain section thickness. BrdU-labeled cells were analyzed for the following phenotypes: BrdU + DCX-positive, BrdU + GFAP-positive, BrdU-positive cells that did not co-localized with either marker. Percentages of cells of each phenotype from the total number of BrdU-positive cells were calculated.

Morphologic evaluation of immature granule cells

Newly born granule cells in the adult DG were immunolabeled using DCX, a marker for immature neurons (Rao and Shetty, 2004; Couillard-Despres, et al., 2005) and examined from bregma -3.0 (for IPB) or -3.3 (for SPB) mm to -4.3 mm. DCX is detectable in the neuronal soma, axons and dendrites and has the highest expression in distal portions of developing processes (Francis, et al, 1999; Friocourt et al., 2003). DCX-positive granule cells were evaluated in both control and Pb²⁺-exposed PN50 rats that had not been previously injected with BrdU to rule out any potential effects of BrdU cytotoxicity on the structure of immature granule cells (Bannigan, 1987; Sekerkova et al., 2004). Morphological features of DCX-positive granule cells were examined at various magnifications and were characterized qualitatively using structural criteria and spatial cell orientation (Ambrogini, et al., 2004; Kempermann et al., 2004; Seri et al., 2004; Rao, et al., 2005).

Estimation of doublecortin-labeled fiber length density

Brain sections were analyzed using Olympus BX51 microscope with an attached Olympus DP70 video camera and motorized stage (Prior Scientific Instruments Ltd, Cambridge, England). Series of every six section (240 μm apart) throughout the extent of the dorsal hippocampus in both control and Pb²⁺-exposed rats were immunolabeled for DCX and all slides were coded prior to microscopic examination. We examined the DCX-positive fibers in

the outer portion of the ML (OML) using global spatial sampling with isotropic virtual planes (Larsen et al., 1998) generated by the CAST-GRID software (Olympus, Denmark). The boundaries of the OML were defined as the outer one third of the ML and outlined digitally using a $\times 4$ objective lens. The focal plane along the section z-axis was measured using ProScan II microcator (Prior Scientific Instruments Ltd, Cambridge, England). Fiber length density was estimated bilaterally using a $\times 100$ oil immersion lens. Sampling boxes with fixed x -, y - and z -parameters were generated by the computer software in a systematic random manner $100\ \mu\text{m}$ (both x - and y -steps) apart and were superimposed on the video images of the microscopic fields that were viewed by changing focal planes throughout the section thickness. Virtual planes generated by the software with a $5\ \mu\text{m}$ sampling plane appeared as lines moving along the z -axis with the focal plane changing and had a different random isotropic orientation for each new counting field. The number of intersects of DCX-labeled fibers with moving lines were counted within the limits of the sampling boxes. Being proportional to the fiber length, these numbers presented a base for estimating length per unit of volume (length-density). The stereological sampling is designed so that at least 150 intersects were counted for each animal. For each of the DG blades, measurements were started at the septo-temporal level where DCX-positive cells were first detected as an intact row of cells, which was section 1 for the IPB and section 2 for SPB.

Timm's staining

To assess whether Pb^{2+} exposure altered mossy fibers terminal fields in the CA3 region of the hippocampus, we used a modified Timm's sulfide/silver method, which allows the visualizing of the zinc distribution in the mossy fiber pathway (Haug et al., 1971; Danscher, 1981; Sloviter, 1982). We have adapted this technique for processing free-floating sections and used additional groups of PN50 rats (control, $n=6$; Pb^{2+} -treated rats, $n=6$) due to differences in fixation protocol. Briefly, rats were transcardially perfused with 50 ml phosphate-buffered saline followed by 200 ml of 0.37% sodium sulfide and 400 ml of 4% paraformaldehyde in 0.1M PB followed by tissue preparation procedure described above. Sections were rinsed in PB, post-fixed in 3% glutaraldehyde for 1hr, excessively rinsed with H_2O , and processed for 20 min with silver-enhancing reagent SE-LM (Aurion, Netherlands). Sections were rinsed, mounted on glass slides, dried and coverslipped using DPX (Fluka).

Analysis of Timm's staining in the CA3 region of the hippocampus

Timm's staining in the hippocampus CA3 region (from bregma $-2.3\ \text{mm}$ to $-4.5\ \text{mm}$) appeared to have a laminar pattern. We analyzed regional differences between control and Pb^{2+} -treated rats in the stratum oriens (SO). The area of Timm's staining in the SO appeared as an outer band and was estimated using unbiased Cavalieri principle (CAST, Olympus, Denmark) every six sections throughout the dorsal hippocampus. To analyze the differences in Timm's staining between treatment groups at the corresponding hippocampal levels, individual profiles of Timm's-positive SO were outlined digitally, the area measured and plotted along the septo-temporal axis. All the measurements were obtained for both sides of the rat brain and averaged.

Statistical Analysis

Statistical analysis for the estimation of BrdU-positive cells in the dorsal DG for both, the proliferation and survival studies, was performed using Poisson regression model (STATA) with cell count as a response variable, reference area as an offset, and experimental group as a factor. This model is a standard statistical method for analyzing count data (Cameron and Trivedi, 1998). Details of Poisson regression analysis can be found in Generalized Linear Models (McCullagh et al., 1989) or in the STATA help section. We also examined differences between treatment groups on BrdU-positive cell counts throughout the extent of the dorsal DG in both the survival and proliferation studies. Cell count was obtained every 6 sections and cell

number per area plotted along the septo-temporal axis of the dorsal DG. These data were analyzed using Two-way ANOVA with treatment and section number as factors and cell number per area as the dependent variable. A similar statistical approach was also used for the volume measurements for Timm's staining and fiber-length density. Where appropriate, differences between treatment groups were compared using student's t-test. Values represent the mean \pm standard error of number of determinations. Statistical significance was set at $p < 0.05$.

RESULTS

Blood Pb²⁺ levels

Whole blood Pb²⁺ concentrations at PN50 were as follows: control (n=15): 0.75 ± 0.11 $\mu\text{g/dL}$ and Pb²⁺-exposed (n=14): 25.8 ± 1.28 $\mu\text{g/dL}$. These blood Pb²⁺ concentrations are similar to our previous studies (Nihei et al., 2000) and are of the same magnitude as those present in certain segments of the population in the United States and throughout the world (Toscano and Guilarte, 2005).

Effect of Pb²⁺ exposure on cell proliferation and cellular fate

One day after the last BrdU injection, newly generated cells in the dorsal DG of both control and Pb²⁺-exposed rats were detected primarily in the SGZ (Figure 2a, b). Compared to mature granule cells, proliferating newly born cells were usually elongated in shape and frequently arranged in clusters (Figure 2a, insert). When compared to controls, the estimated total number of proliferating BrdU-positive cells in the dorsal DG of Pb²⁺-exposed rats was decreased by 13% (mean \pm sem: Controls: $11,493 \pm 1319$, Pb²⁺-exposed: $10,035 \pm 554$; $p < 0.001$). When the data was plotted as the number of BrdU-positive cells per unit area along the septo-temporal axis of the dorsal hippocampus (Figure 2c), there was a highly significant treatment effect ($F_{1,96} = 6.11$; $p < 0.02$) with no effect of section number along the septo-temporal axis ($F_{6,96} = 0.31$; $p > 0.05$) or interaction ($F_{6,96} = 0.39$; $p > 0.05$).

Co-labeling of BrdU with DCX or GFAP (Figure 3a,b) confirmed that the vast majority of BrdU-positive cells in both control and Pb²⁺-exposed rats either had an immature neuronal phenotype based on co-labeling with DCX (controls: $78.8 \pm 4.4\%$ of 277 examined cells; Pb²⁺-exposed $77.2 \pm 6.9\%$ of 255 examined cells) or did not co-localize with either DCX or GFAP (19.8 ± 4.0 and $21.0 \pm 6.8\%$ for control and Pb²⁺-exposed rats, respectively) and likely represented undifferentiated newborn cells. A small percentage of BrdU-labeled cells co-localized with GFAP (control: $1.34 \pm 0.84\%$; Pb²⁺-exposed: $1.79 \pm 0.6\%$), although astrocytic processes were commonly observed in close proximity to BrdU + DCX-positive cells. These findings indicate that chronic exposure to Pb²⁺ did not alter the cellular fate of newly born cells.

Effect of Pb²⁺ exposure on survival of newly generated granule cells

Four weeks after the last BrdU administration, BrdU labeled cells were typically detected within the inner portion of the GCL (Figure 4 a,b). When compared to controls, the total estimated number of BrdU-positive cells in the GCL in the dorsal DG of Pb²⁺-exposed rats decreased by 22.7% (mean \pm sem, controls- 5993 ± 345 , Pb²⁺-exposed- 4630 ± 393 ; $p < 0.001$). When the data was plotted as the number of BrdU-positive cells per unit area along the septo-temporal axis of the dorsal hippocampus (Figure 4c), there was a highly significant treatment effect ($F_{1,54} = 24.4$; $p < 0.001$) with no effect of section number on the number of BrdU-positive cells along the septo-temporal axis ($F_{5,54} = 2.26$; $p > 0.05$) or interaction ($F_{5,54} = 0.08$; $p > 0.05$).

Effect of Pb²⁺ exposure on dendritic morphology of immature granule cells

DCX-positive cells were distributed throughout the extent of the DG in both control and Pb²⁺-exposed rats (Figure 5a, b) and comprised a morphologically heterogeneous population of granule neurons at different stages of differentiation. The length and pattern of the dendritic arborization has been considered to correlate with the degree of granule cell maturation (Ambrogini, et al., 2004; Kempermann et al., 2004; Seri et al., 2004; Rao, et al., 2005; Zhao et al., 2006). In control animals, DCX-positive granule cell at different stages of development seemed to be evenly distributed forming a relatively homogeneous cell population (Figure 5a). The majority of the DCX-positive cells were uniformly oriented and had apical dendrites bifurcating within the outer half of the GCL and further branching within the inner portion of the ML (Figure 5a). Fine dendritic terminals extended throughout the DG-ML reaching the hippocampal commissure (Figure 5a). Compared to controls, the population of DCX-positive granule cells in the DG of Pb²⁺-exposed rats was morphologically more heterogeneous due to alterations in the orientation of their dendritic structure (Figures 5b and 6b). We commonly observed irregularly oriented granule cells apical dendrites with reduced dendritic branching, or cells with shorter primary dendrites bifurcating in close proximity to the neuronal soma and forming dendritic arbors with a “bushy” appearance within the GCL (Figure 5b and 6 b,c). In Pb²⁺-exposed rats, we also observed DCX-labeled dendrites that were short and convoluted with a “spiral-like” appearance resembling dystrophic dendrites (See Figure 6c and d). Overall, dendrites of DCX-positive cells in the DG of Pb²⁺-exposed rats appeared shorter since their terminals extended only into the inner ML (IML) or medial aspect of the ML (MML), with significantly less innervation of the outer ML (OML) (Figures 5b and d).

Effect of Pb²⁺ exposure on dendritic length density of immature granule cells

Based on the above findings, we measured the length density of DCX-positive dendrites extending into the OML of the DG. In the OML of the SPB of Pb²⁺-exposed rats, the length-density of the DCX-labeled fibers was significantly reduced (on average by 36%) relative to controls (mean \pm sem: controls-3910 \pm 336 (n=6) and Pb²⁺-exposed-2505 \pm 289 (n=6) $\mu\text{m} \times 10^{-7} / \mu\text{m}^3$, $p < 0.0001$). The decrease in DCX-positive fibers length density observed in the SPB of Pb²⁺-exposed rats was present along the entire septo-temporal axis of the dorsal DG (Figures 5e). When the SPB data were plotted as the length density along the septo-temporal axis of the dorsal hippocampus (Figure 5e), there was a highly significant treatment effect ($F_{1,39} = 21.8$; $p < 0.001$) with no effect of section number on the length density of DCX-positive length density ($F_{3,39} = 1.55$; $p > 0.05$) or interaction ($F_{3,39} = 0.69$; $p > 0.05$). Importantly, in the IPB, no significant differences were noted (control-4364 \pm 341 (n=6) and Pb²⁺-exposed-3821 \pm 238 (n=6) $\mu\text{m} \times 10^{-7} / \mu\text{m}^3$, $p = 0.1293$) (Figure 5f).

Timm's staining in the CA3 region of the hippocampus

We observed significant differences in Timm's staining between control and Pb²⁺-exposed rats in the CA3 region of the hippocampus, in particular, in the subregion corresponding to the stratum oriens (SO) (Figure 7 a,b). Volume estimation of Timm's staining in the CA3-SO using the Cavalieri method revealed a 26% decrease in volume in Pb²⁺-treated rats relative to controls (mean \pm sem: control-0.1816 \pm 0.0275 (n=6) and Pb²⁺-exposed-0.1341 \pm 0.0119 mm³ (n=6), $p < 0.05$). The distribution of individual area measurements for Timm's staining along the septo-temporal axis (Figure 7c) showed highly significant treatment ($F_{1,93} = 4.85$; $p < 0.001$) and section number ($F_{10,93} = 34.0$; $p < 0.001$) effects with no significant interaction ($F_{10,93} = 0.82$; $p > 0.05$).

DISCUSSION

The main finding of the present study is that chronic exposure to environmentally relevant levels of Pb²⁺ during early life alters granule cell neurogenesis and morphology in the DG of

young adult rats. We show that Pb^{2+} exposure decreased the proliferation of newly generated cells but did not alter their cellular fate. Further, it decreased the survival of newly born granule cells and altered their morphology manifested by reductions in the length density of DCX-labeled apical dendrites and in the Timm's positive mossy fiber terminal fields in the CA3 region. It should be noted that a limitation of the experimental design used in the present study is that Pb^{2+} exposure occurred continuously during gestation and throughout the postnatal period until the animals were tested as young adults. Therefore, we do not know if the effects of Pb^{2+} on adult neurogenesis are specific to a defined stage of development, which will be investigated in future studies.

The decrease in granule cell proliferation in the DG documented in our study is in agreement with reports in which exposure to Pb^{2+} produced an inhibitory effect on neurosphere proliferation (Huang and Schneider, 2004; Schneider et al., 2005). As these authors point out, one potential mechanism of Pb^{2+} -induced decrease on progenitor cell proliferation may be due to its inhibitory effects on DNA binding of zinc finger transcription factors such as Sp1 and TFIIIA (Zawia et al., 1998; Hanas et al., 1999). An alternative mechanism by which chronic Pb^{2+} exposure alters granule cell neurogenesis may be related to alterations in NMDAR function (Nacher and McEwen, 2006). Pb^{2+} is a potent and selective inhibitor of the NMDAR (Alkondon et al., 1990; Guilarte and Miceli, 1992; Gavazzo et al., 2001) and chronic exposure to Pb^{2+} has been documented to alter NMDAR subunit expression and composition in the hippocampus of young adult rats (Guilarte and McGlothan, 1998; Nihei and Guilarte 1999; Guilarte et al., 2000; Nihei et al., 2000; Toscano et al., 2002; Zhang et al., 2002). Pb^{2+} -induced alterations in NMDAR composition modify downstream signaling pathways leading to decreased CREB phosphorylation and binding activity (Toscano et al., 2003; Toscano and Guilarte, 2005) and may be linked to the effects on granule cell neurogenesis observed in the present study. In this context, it has been recently shown that the survival of new neurons in the DG is partly regulated by cell-specific activation of NMDAR during a short period soon after birth. That is, cell-specific knock out of the NR1 subunit of the NMDAR in newly born cells of the DG reduced their survival (Tashiro et al., 2006).

The Pb^{2+} -induced decrease in granule cell neurogenesis observed in our study is likely to have detrimental effects on neuronal circuits in the hippocampus at both the structural and functional levels. For example, a reduction in the number of newly born granule cells may influence mossy fibers innervation of the CA3 region, altering neuronal connectivity, pyramidal cell excitability and memory formation (Trevers and Rolls, 1994; Kempermann and Wiscott, 2004; Kesner et al., 2004). Consistent with this notion, we found that Pb^{2+} -exposed rats exhibited a decrease in the total area of Timm's staining in the CA3-SO suggesting that the deficits in neurogenesis may be associated with a decrease in mossy fibers innervation to this region.

Mossy fiber innervation of the CA3-SO has been associated with spatial learning performance (Lasalle et al., 2000; Ramirez-Amaya et al., 2001; Holahan et al., 2006). Inactivation of mossy fibers by the zinc chelator diethyldithiocarbamate disrupted spatial learning (Lasalle et al., 2000) while extensive water maze training enhanced the performance of rodents in the water maze test and this effect positively correlated with increased Timm's staining in the CA3-SO (Ramirez-Amaya et al., 2001; Holahan et al., 2006). These observations provide an important link between spatial learning performance and the remodeling of mossy fiber synapses in the CA3-SO. They are consistent with our observations that young adult rats chronically exposed to Pb^{2+} have reduced Timm's staining in the CA3-SO (present study) and they exhibit deficits in spatial learning (Nihei et al., 2000; Guilarte et al., 2003).

Chronic Pb^{2+} exposure also affected granule cell morphology. Fine apical dendrites of newly born granule cells in Pb^{2+} -exposed rats were significantly reduced in the OML of the DG. Dendrites frequently appeared dystrophic, similar to those present in aging rats (Rao et al.,

2005), Alzheimer's disease (Flood et al., 1986;De Ruiter, 1987), after entorhinal/fimbria fornix lesion (Schauwecker and McNeill, 1996) and in chronic alcohol exposure (He et al., 2005). Dendrites play an essential role in neuronal signaling (Barinaga, 1995) and aberrations in dendritic morphology are likely to alter their functional characteristics (Kaech et al., 1996;Kaufmann et al., 2000). The size of cell bodies and the complexity of the dendritic tree in maturing granule cells have been shown to correlate with changes in their electrophysiological properties (Liu et al., 2000;Ambrogini, 2004). The relevance of this morpho-functional association was also demonstrated by the relationship between the extent of the dendritic tree and type of synaptic input. GABAergic input is limited to the thickness of the GCL, while glutamatergic input is associated with apical dendrite terminals extending through the ML of the DG (Ye et al., 2000). Granule cell dendritic spines are the major sites for glutamatergic input from the perforant path. Therefore, the timing of spine formation in the outer aspects of the ML reflects one of the important transitions in maturation of the physiological function of granule cells (Zhao et al., 2006). Pb^{2+} -induced reductions in the length density of apical dendrites in the OML may influence the electrophysiological properties of glutamatergic synapses and their plasticity (Snyder et al., 2001) and are consistent with reports that Pb^{2+} -exposed rats exhibit deficits in perforant path-DG LTP (Lasley et al., 1993;Gilbert et al., 1996;Gilbert and Mack, 1998;Nihei et al., 2000).

The precise mechanisms by which Pb^{2+} exposure alters the dendritic development of granule cells are not currently known. We have recently documented a reduction in CaMKII activity with a specific decrease in CaMKII- β protein with no change in CaMKII- α in the hippocampus of rats of similar age and Pb^{2+} treatment as those in the present study (Toscano et al., 2005). This finding provides a potential explanation to the present results since changes in CaMKII- β expression has a direct effect on the movement, extension and branching of filopodia and fine dendrites as well as synapse formation (Fink et al., 2003).

In summary, chronic exposure to Pb^{2+} , a ubiquitous environmental pollutant and neurotoxicant, has detrimental effects on granule cell proliferation, survival and morphology in the DG altering the cytoarchitecture of the rat hippocampus. These findings provide a cellular and morphological basis for the deficits in hippocampal LTP and spatial learning documented in Pb^{2+} -exposed animals.

Acknowledgements

This work was supported by grant number ES06189 to TRG from the National Institute of Environmental Health Sciences. The authors give thanks to Dr. Mary Blue for assistance with the MicroBrightField Stereology System.

References

- Abrous DN, Koehl M, Le Moal M. Adult neurogenesis: from precursors to network and physiology. *Physiol Rev* 2005;85:523–569. [PubMed: 15788705]
- Alkondon M, Costa AC, Radhakrishnan V, Aronstam RS, Albuquerque EX. Selective blockade of NMDA-activated channel currents may be implicated in learning deficits caused by lead. *FEBS Lett* 1990;261:124–130. [PubMed: 1689669]
- Ambrogini P, Lattanzi D, Ciuffoli S, Agostini D, Bertini L, Stocchi V, Santi S, Cuppini R. Morpho-functional characterization of neuronal cells at different stages of maturation in granule cell layer of adult rat dentate gyrus. *Brain Res* 2004;1017:21–31. [PubMed: 15261095]
- Arvidsson A, Kokaia Z, Lindvall O. N-methyl-D-aspartate receptor-mediated increase of neurogenesis in adult dentate gyrus following stroke. *Eur J Neurosci* 2001;14:10–18. [PubMed: 11488944]
- Bannigan JG. Autoradiographic analysis of effects of 5-bromodeoxyuridine on neurogenesis in the chick embryo spinal cord. *Brain Res* 1987;433:161–170. [PubMed: 3690329]
- Barinaga M. Dendrites shed their dull image. *Science* 1995;268:200–201. [PubMed: 7536341]

- Barnabeu R, Sharp FR. NMDA and AMPA/kainate glutamate receptors modulate dentate neurogenesis and CA3 synapsin-I in normal and ischemic hippocampus. *J Cereb Blood Flow* 2000;20:1669–1680.
- Cameron HA, McEwen BS, Gould E. Regulation of adult neurogenesis by excitatory input and NMDA receptor activation in the dentate gyrus. *J Neurosci* 1995;15:4687–4692. [PubMed: 7790933]
- Cameron, AC.; Trivedi, PK. *Regression Analysis of Categorical Data*. Cambridge University Press; 1998.
- Chun SK, Sun W, Park J-J, Jung MW. Enhanced proliferation of progenitor cells following long-term potentiation induction in the rat dentate gyrus. *Neurobiol Learning Memory* 2006;86:322–329.
- Couillard-Despres S, Winner B, Schaubeck S, Ainger R, Vroemen M, Weidner N, Bogdahn U, Winkler J, Kuhn H, Aigner L. Doublecortin expression levels in adult brain reflects neurogenesis. *Eur J Neurosci* 2005;21:1–14. [PubMed: 15654838]
- Danscher G. Histochemical demonstration of heavy metals. A revised method suitable for both light and electron microscopy. *Histochem* 1981;71:1–16.
- de Ruiter P, Uylings HB. Morphometric and dendritic analysis of fascia dentata granule cells in human aging and senile dementia. *Brain Res* 1987;402:217–229. [PubMed: 3828794]
- Deisseroth K, Singla S, Toda H, Monje M, Palmer T, Malenka RC. Excitation-neurogenesis coupling in adult neural stem/progenitor cells. *Neuron* 2004;42:535–552. [PubMed: 15157417]
- Drapeau E, Mayo W, Aurousseau C, Le Moal M, Piazza P-V, Abrous DN. Spatial memory performance of aged rats in the water maze predicts level of hippocampal neurogenesis. *Proc Nat Acad Sci* 2003;100:14385–14390. [PubMed: 14614143]
- Fink CC, Bayer KU, Myers JW, Ferrell JE, Schulman H, Meyer T. Selective regulation of neurite extension and synapse formation by the beta but not the alpha isoform of CaMKII. *Neuron* 2003;39:283–297. [PubMed: 12873385]
- Flood DG, Coleman PD. Failed compensatory dendritic growth as a pathophysiological process in Alzheimer's disease. *Can J Neurol Sci* 1986;13:475–479. [PubMed: 3791064]
- Francis F, Koulakoff A, Boucher D, Chafey P, Schaar B, Vinet M, Friocourt G, McDonnell N, Reiner O, Kahn A, McConnell SK, Berwald-Netter Y, Denoulet P, Chelly J. Doublecortin is a developmentally regulated, microtubule-associated protein expressed in migrating and differentiating neurons. *Neuron* 1999;23:247–256. [PubMed: 10399932]
- Friocourt G, Koulakoff A, Chafey P, Boucher D, Fauchereau F, Chelly J, Francis F. Doublecortin functions at the extremities of growing neuronal processes. *Cer Cortex* 2003;13:620–626.
- Gavazzo P, Gazzoli A, Mazzolini M, Marchetti C. Lead inhibition of NMDA channels in native and recombinant receptors. *NeuroReport* 2001;12:3121–3125. [PubMed: 11568649]
- Gilbert ME, Mack CM. Chronic lead exposure accelerates decay of long-term potentiation in rat dentate gyrus in vivo. *Brain Res* 1998;789:139–149. [PubMed: 9602098]
- Gilbert ME, Mack C, Lasley S. Chronic developmental lead exposure increases the threshold for long-term potentiation in rat dentate gyrus in vivo. *Brain Res* 1996;736:118–124. [PubMed: 8930316]
- Gould E. The effects of adrenal steroids and excitatory input on neuronal birth and survival. *Ann N Y Acad Sci* 1994;743:73–92. [PubMed: 7802420]
- Gould E, McEwen BS, Tanapat P, Galea LA, Fuchs E. Neurogenesis in the dentate gyrus of the adult tree shrew is regulated by psychosocial stress and NMDA receptor activation. *J Neurosci* 1997;17:2492–2498. [PubMed: 9065509]
- Guilarte TR, McGlothlan JL. Hippocampal NMDA receptor mRNA undergoes subunit specific changes during developmental lead exposure. *Brain Res* 1998;790:98–107. [PubMed: 9593842]
- Guilarte TR, Miceli RC. Age-dependent effects of lead on [³H]-MK-801 binding to the NMDA receptor-gated ionophore: In vitro and in vivo studies. *Neurosci Lett* 1992;148:27–30. [PubMed: 1300499]
- Guilarte TR, McGlothlan JL, Nihei MK. Hippocampal expression of N-methyl-D-aspartate receptor. NMDAR1 subunit splice variant mRNA is altered by developmental exposure to Pb²⁺ *Brain Res Mol Brain Res* 2000;76:299–305. [PubMed: 10762705]
- Guilarte TR, Toscano CD, McGlothlan JL, Weaver SA. Environmental enrichment reverses cognitive and molecular deficits induced by developmental lead exposure. *Ann Neurol* 2003;53:50–56. [PubMed: 12509847]
- Hanas JS, Rodgers JS, Bantle JA, Cheng YG. Lead inhibition of DNA-binding mechanisms of Cys₂His₂ zinc finger proteins. *Mol Pharm* 1999;56:982–988.

- Haug FM, Blackstad TW, Simonsen AH, Zimmer J. Timm's sulfide silver reaction for zinc during experimental anterograde degeneration of hippocampal mossy fibers. *J Comp Neurol* 1971;142:23–31. [PubMed: 4103052]
- He J, Nixon K, Shetty AS, Crews FT. Chronic alcohol exposure reduces hippocampal neurogenesis and dendritic growth in newborn neurons. *Eur J Neurosci* 2005;21:2711–2720. [PubMed: 15926919]
- Holahan MR, Rekart JL, Sandoval J, Routtenberg A. Spatial learning induces presynaptic structural remodeling in the hippocampal mossy fiber system of two rat strains. *Hippocampus* 2006;16:560–570. [PubMed: 16685708]
- Huang F, Schneider JS. Effects of lead exposure on proliferation and differentiation of neural stem cells derived from different regions of embryonic rat brain. *Neurotoxicol* 2004;25:1001–1012.
- Kaech S, Ludin B, Matus A. Cytoskeletal plasticity in cells expressing neuronal microtubule-associated proteins. *Neuron* 1996;17:1189–1199. [PubMed: 8982165]
- Kaufmann WE, Moser HW. Dendritic anomalies in disorders associated with mental retardation. *Cereb Cortex* 2000;10:981–991. [PubMed: 11007549]
- Kempermann, G.; Wiskott, L. What is the functional role of new neurons in the adult dentate gyrus? *Proc Stem cells in the nervous system: Functional and clinical implications*. In: Gage, FH.; Björklund, A.; Prochiantz, A.; Christen, Y., editors. Research and Perspectives in Neurosciences Foundation Ipsen. Springer; Berlin: 2004. p. 57-65. Paris, January 20, 2003
- Kempermann G, Wiskott L, Gage FH. Functional significance of adult neurogenesis. *Curr Opin Neurobiol* 2004;14:186–191. [PubMed: 15082323]
- Kesner RP, Lee I, Gilbert P. A behavioral assessment of hippocampal function based on a subregional analysis. *Rev Neurosci* 2004;15:333–351. [PubMed: 15575490]
- Larsen JO, Gundersen HJG, Nielsen J. Global spatial sampling with isotropic virtual planes: estimators of length density and total length in thick, arbitrary oriented sections. *J Microscopy* 1998;191:238–248.
- Lasley SM, Polan-Curtain J, Armstrong DL. Chronic exposure to environmental levels of lead impairs in vivo induction of long-term potentiation in rat hippocampal dentate. *Brain Res* 1993;614:347–351. [PubMed: 8348326]
- Lassalle J-M, Bataille T, Halley H. Reversible inactivation of the hippocampal mossy fiber synapse in mice impairs spatial learning but neither consolidation nor memory retrieval, in the Morris navigation task. *Neurobiol Learn Memory* 2000;73:243–257.
- Liu X, Tilwalli S, Ye G, Lio P, Pasternak JF, Trommer BL. Morphologic and electrophysiologic maturation in developing dentate gyrus granule cells. *Brain Res* 2000;856:202–212. [PubMed: 10677627]
- Lynch MA. Long-term potentiation and memory. *Physiol Rev* 2004;84:87–136. [PubMed: 14715912]
- Mc Cullagh, P.; Nadler, SA. *Generalized linear models*. 2. Chapman and Hall; London: 1989.
- Nacher J, Alonso-Llosa G, Rosell DR, McEwen BS. NMDA receptor antagonist treatment increases the production of new neurons in the aged rat hippocampus. *Neurobiol Aging* 2003;24:273–284. [PubMed: 12498961]
- Nacher J, McEwen BS. The role of *N*-methyl-d-aspartate receptors in neurogenesis. *Hippocampus* 2006;16:267–270. [PubMed: 16425227]
- Nakazawa K, McHugh T, Wilson M, Tonegawa S. NMDA receptors, place cells and hippocampal spatial memory. *Nat Rev Neurosci* 2004;5:361–372. [PubMed: 15100719]
- Nihei MK, Guilarte TR. NMDAR-2A subunit protein expression is reduced in the hippocampus of rats exposed to Pb²⁺ during development. *Brain Res Mol Brain Res* 1999;66:42–49. [PubMed: 10095076]
- Nihei MK, Desmond NL, McGlothan JL, Kuhlmann AC, Guilarte TR. *N*-methyl-D-aspartate receptor subunit changes are associated with lead-induced deficits of long-term potentiation and spatial learning. *Neurosci* 2000;99:233–242.
- Nowakowski RS, Lewin SB, Miller MW. Bromodeoxyuridine immunohistochemical determination of the lengths of the cell cycle and the DNA-synthetic phase for an anatomically defined population. *J Neurocytol* 1989;18:311–318. [PubMed: 2746304]

- Parent JM, Yu TW, Leibowitz RT, Geschwind DH, Sloviter RS, Lowenstein DH. Dentate granule cell neurogenesis is increased by seizures and contributes to aberrant network reorganization in the adult rat hippocampus. *J Neurosci* 1997;17:3727–3738. [PubMed: 9133393]
- Ramirez-Amaya V, Balderas I, Sandoval J, Escobar ML, Bermudez-Rattoni F. Spatial long-term memory is related to mossy fiber synaptogenesis. *J Neurosci* 2001;15:7340–7348. [PubMed: 11549744]
- Rao MS, Shetty AK. Efficacy of doublecortin as a marker to analyse the absolute number and dendritic growth of newly generated neurons in the adult dentate gyrus. *Eur J Neurosci* 2004;19:234–246. [PubMed: 14725617]
- Rao MS, Hattiangady B, Abdel-Rahman A, Stanley DP, Shetty AK. Newly born cells in the ageing dentate gyrus display normal migration, survival and neuronal fate choice but endure retarded early maturation. *Eur J Neurosci* 2005;21:464–476. [PubMed: 15673445]
- Schauwecker PE, McNeill TH. Dendritic remodeling of dentate granule cells following a combined entorhinal cortex/fimbria fornix lesion. *Exp Neurol* 1996;141:145–153. [PubMed: 8797677]
- Schneider JS, Anderson DW, Wade TV, Smith MG, Leibrandt P, Zuck L, Lidsky TI. Inhibition of progenitor cell proliferation in the dentate gyrus of rats following post-weaning lead exposure. *Neurotoxicol* 2005;26:141–145.
- Sekerková G, Ilijic E, Mugnaini E. Bromodeoxyuridine administered during neurogenesis of the projection neurons causes cerebellar defects in rat. *J Comp Neurol* 2004;470:221–239. [PubMed: 14755513]
- Seri B, García-Verdugo JM, Collado-Morente L, McEwen BS, Alvarez-Buylla A. Cell types, lineage, and architecture of the germinal zone in the adult dentate gyrus. *J Comp Neurol* 2004;478:359–378. [PubMed: 15384070]
- Sloviter RS. A simplified Timm stain procedure compatible with formaldehyde fixation and routine paraffin embedding of rat brain. *Brain Res Bull* 1982;8:771–774. [PubMed: 6182964]
- Snyder JS, Kee N, Wojtowicz JM. Effects of adult neurogenesis on synaptic plasticity in the rat dentate gyrus. *J Neurophysiol* 2001;85:2423–2431. [PubMed: 11387388]
- Suzuki M, Nelson AD, Eickstaedt JB, Wallace K, Wright LS, Svendsen CN. Glutamate enhances proliferation and neurogenesis in human neural progenitor cell cultures derived from fetal cortex. *Eur J Neurosci* 2006;24:645–653. [PubMed: 16848797]
- Tashiro A, Sandler VM, Toni N, Zhao C, Gage FH. NMDA-receptor-mediated, cell-specific integration of new neurons in adult dentate gyrus. *Nature* 2006;442:929–933. [PubMed: 16906136]
- Toscano CD, Guilarte TR. Lead neurotoxicity: From exposure to molecular effects. *Brain Res Rev* 2005;49:529–554. [PubMed: 16269318]
- Toscano CD, Hashemzadeh-Gargari H, McGlothan JL, Guilarte TR. Developmental Pb²⁺ exposure alters NMDAR subtypes and reduces CREB phosphorylation in the rat brain. *Brain Res Dev Brain Res* 2002;139:217–226.
- Toscano CD, McGlothan JL, Guilarte TR. Lead exposure alters cyclic-AMP response element binding protein phosphorylation and binding activity in the developing rat brain. *Brain Res Dev Brain Res* 2003;145:219–228.
- Treves A, Rolls ET. Computational analysis of the role of the hippocampus in memory. *Hippocampus* 1994;4:374–391. [PubMed: 7842058]
- Ye GL, Song Liu X, Pasternak JF, Trommer BL. Maturation of glutamatergic neurotransmission in dentate gyrus granule cells. *Brain Res Dev Brain Res* 2000;124:33–42.
- Zawia NH, Sharan R, Brydie M, Oyama T, Crumpton T. Sp1 as a target for metal-induced perturbations of transcriptional regulation of developmental brain gene expression. *Dev Brain Res* 1998;107:291–298. [PubMed: 9593950]
- Zhang X-Y, Liu A-P, Ruan D-Y, Liu J. Effects of developmental lead exposure on the expression of specific NMDA receptor subunit mRNAs in the hippocampus of neonatal rats by digoxigenin-labeled in situ hybridization histochemistry. *Neurotoxicol Teratol* 2002;24:149–160.
- Zhao C, Teng EM, Summers RG, Ming G-L, Gage FH. Distinct morphological stages of dentate granule neuron maturation in the adult mouse hippocampus. *J Neurosci* 2006;26:3–11. [PubMed: 16399667]

LIST OF ABBREVIATIONS

BrdU	bromodeoxyuridine
DAB	3,3'-diaminobenzidine
DCX	doublecortin
DG	dentate gyrus
GCL	granule cell layer
GFAP	glial fibrillary acidic protein
IPB	infrapyramidal blade
IML	inner molecular layer
LTP	long-term potentiation
ML	molecular layer
NMDAR	<i>N</i> -methyl- <i>d</i> -aspartate receptor
OML	outer molecular layer
PB	phosphate buffer
Pb²⁺	lead
PN	postnatal day
SGZ	subgranular zone
SL	stratum lucidum
SO	stratum oriens
SP	stratum pyramidale

SPB suprapyramidal blade
TBS tris-buffered saline

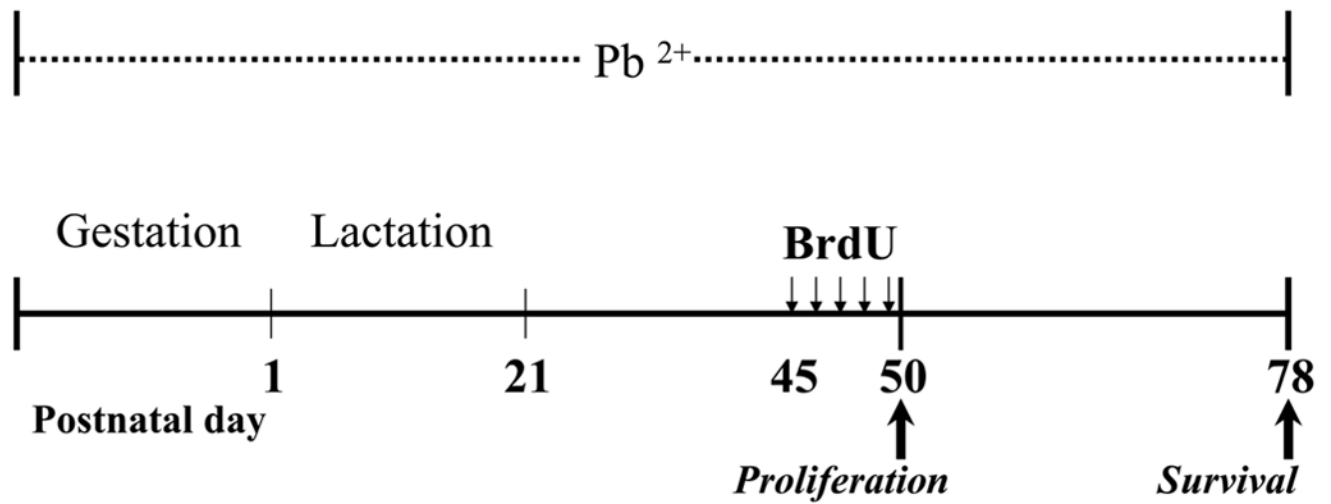


Figure 1. Experimental design and timeline of Pb^{2+} exposure and BrdU administration.

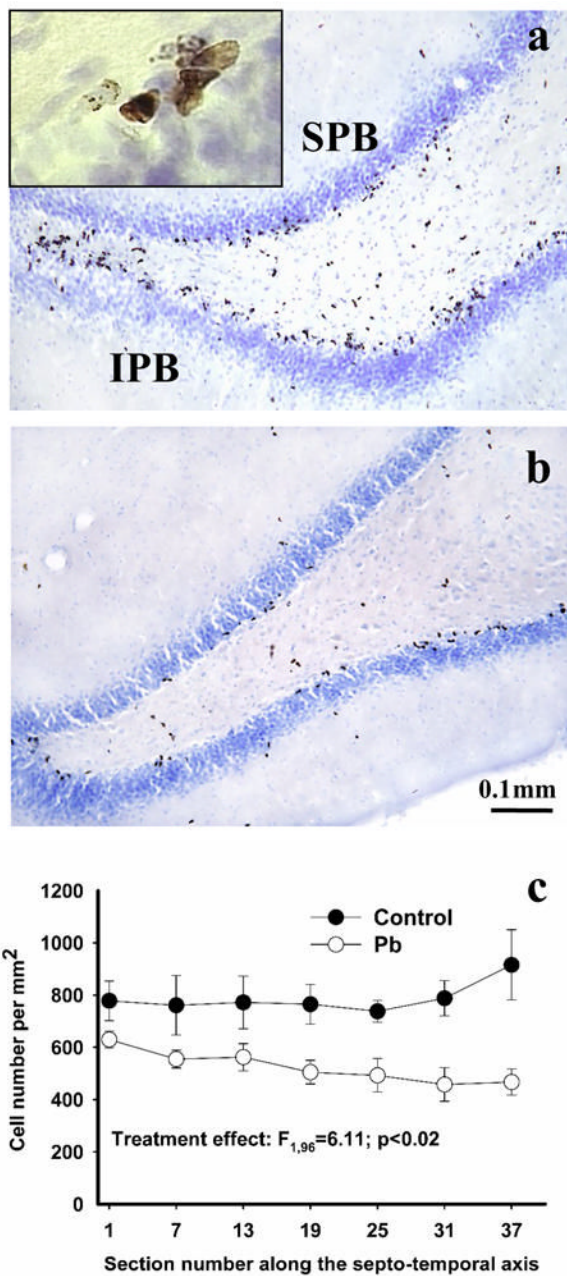


Figure 2. Effect of Pb^{2+} exposure on cell proliferation in the hippocampus DG. The figure depicts BrdU-positive cells one day after the last BrdU administration in the DG of a control (a) and Pb^{2+} -exposed (b) rat. BrdU labeled cells were often arranged in clusters (Figure 2a, insert). A lower number of BrdU labeled cells was detected throughout the entire extent of the dorsal dentate gyrus (c). Each value is the mean \pm sem of $n=7$ different control animals and $n=9$ Pb^{2+} -exposed animals. SPB= suprapyramidal blade; IPB= infrapyramidal blade.

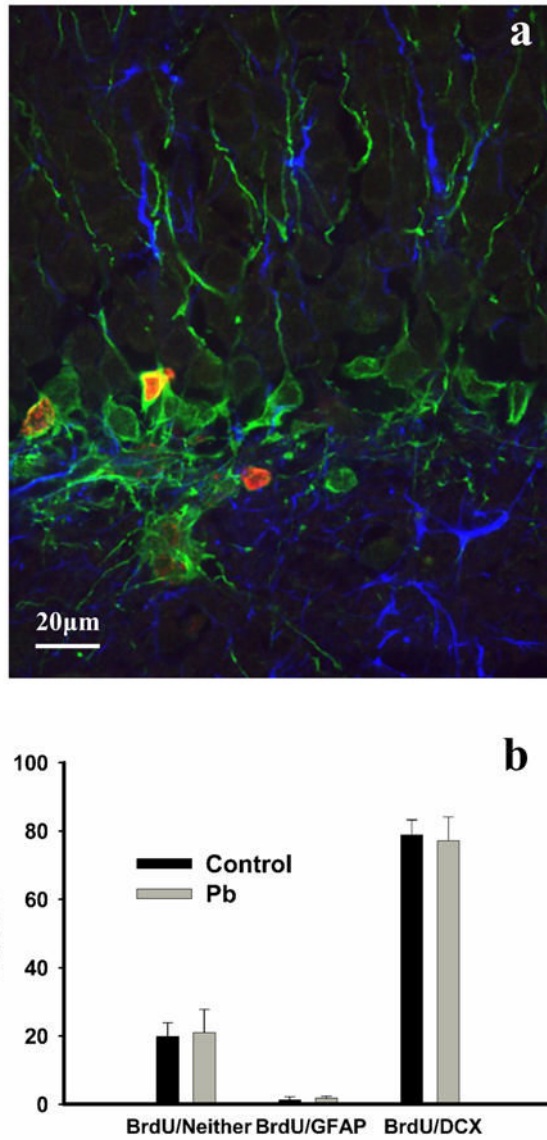


Figure 3.

(a) Co-localization of BrdU (red) with DCX (green) and GFAP (blue). (b) No significant differences in percent co-localization were found between the treatment groups in the percentages of new cells labeled with either a neuronal or astrocytic phenotype. Approximately 20% of cells in control or Pb²⁺-exposed rats did not co-localize with either marker. Mean values were obtained from a total of 4 different animals from both control and Pb²⁺-exposed groups.

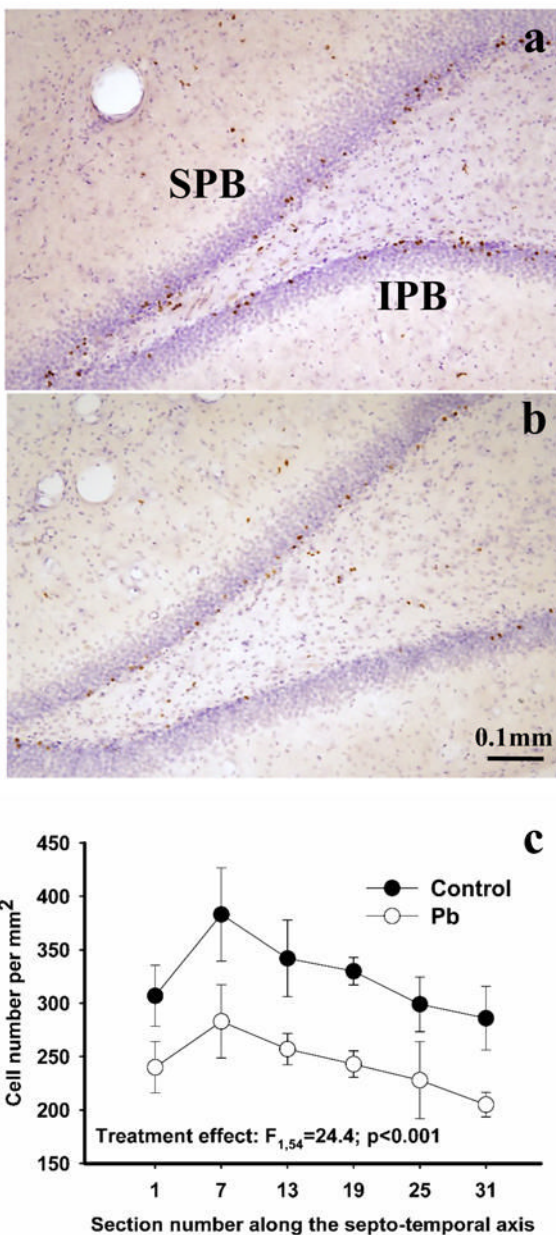


Figure 4. Effect of Pb²⁺ exposure on granule cell survival in the dorsal DG. The figure depicts BrdU-positive cells four weeks after the last BrdU administration in the DG of a control (a) and Pb²⁺-exposed (b) rat. A reduction in the number of BrdU labeled cells was observed throughout the extent of the dorsal DG (c). Each value is the mean ± sem of n=6 different control animals and n=5 Pb²⁺-exposed animals. SPB= suprapyramidal blade; IPB= infrapyramidal blade.

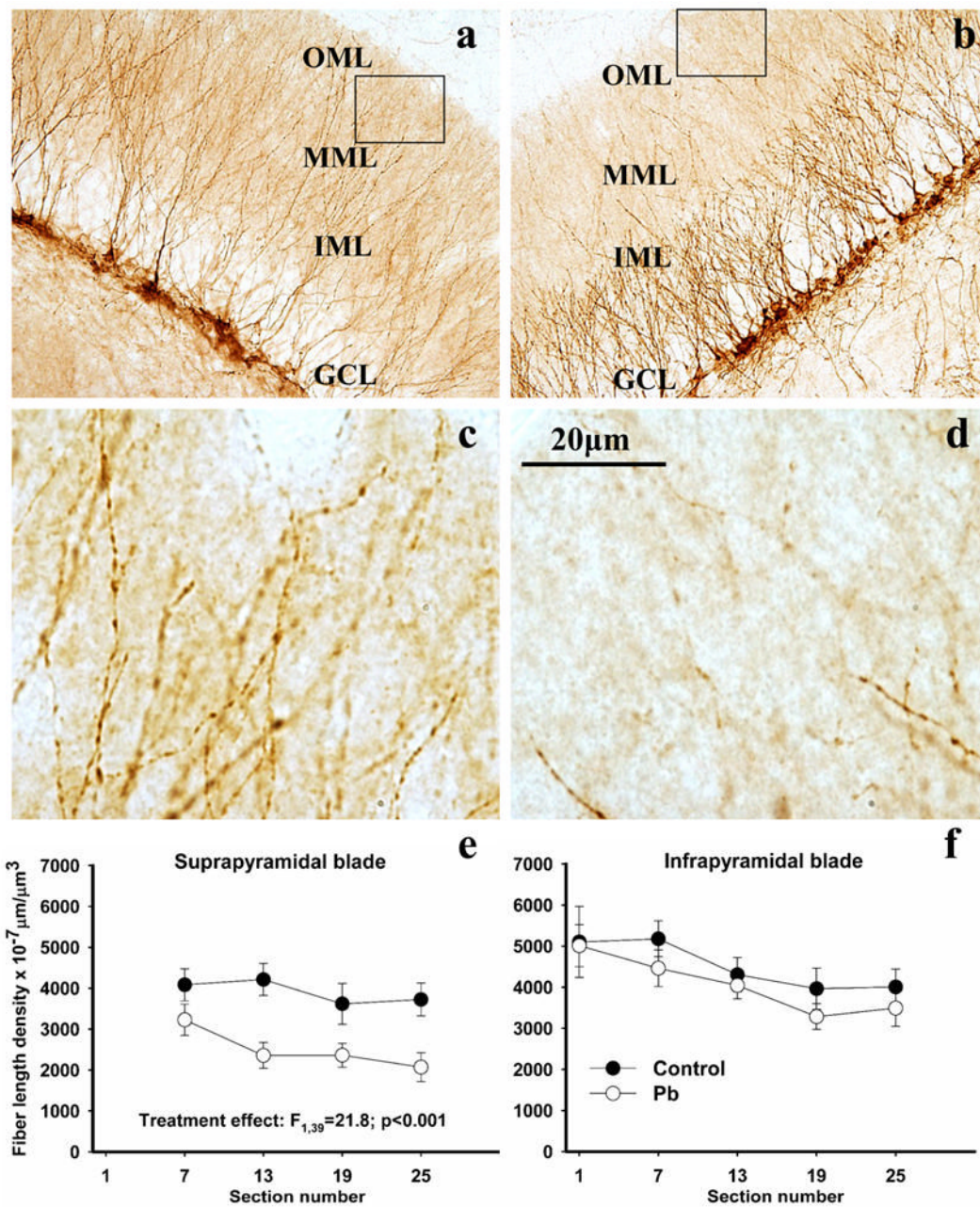


Figure 5.

DCX-positive neurons in the dorsal DG (a,b) and their fiber length densities in the outer molecular layer of the dentate gyrus (c,d) in control and Pb²⁺-exposed rats. Boxed areas in (a) and (b) are represented in (c) and (d) at higher magnification. In control animals (a) DCX-positive neurons displayed vertically oriented primary dendrites that branch within the IML, extending their fine dendrites into the OML generally reaching the hippocampal commissure. In Pb²⁺-treated rats (b), primary dendrites of DCX-positive neurons appeared shorter and formed their arbors within the GCL proper. Their fine terminals generally reached the IML or MML but rarely the OML. In Pb²⁺-exposed rats, the density of the DCX-labeled fiber length was diminished in the OML of the suprapyramidal blade throughout the dorsal DG (f). This effect was not observed in the infrapyramidal blade (e). Each value is the mean ± sem of n=6

different control animals and n=6 Pb^{2+} -exposed animals. OML= outer molecular layer; MML= medial molecular layer; IML= inner molecular layer.

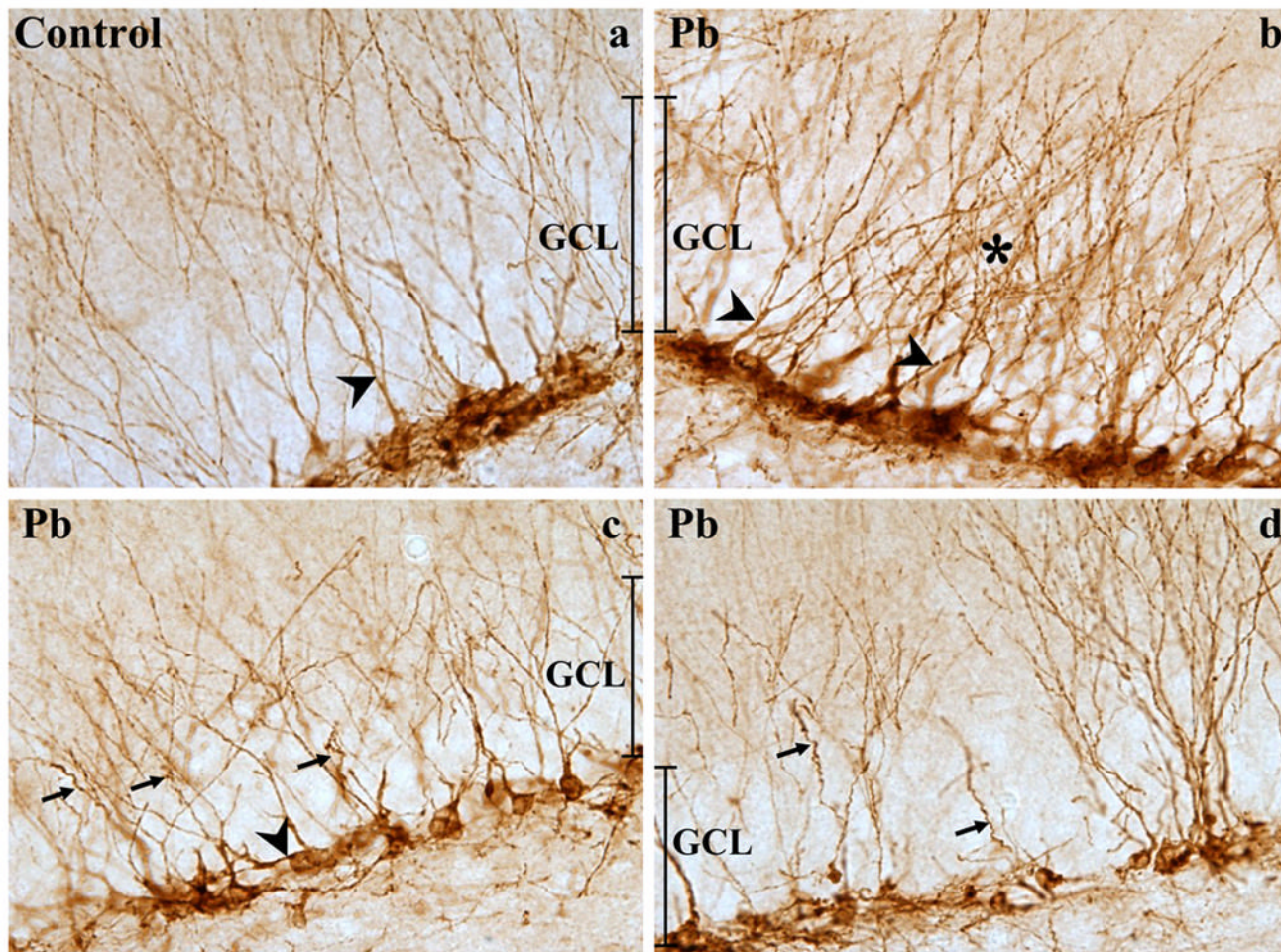


Figure 6.

Representative images of DCX-positive newly born cell morphology in the dorsal DG of control (a) and Pb^{2+} -exposed rats (b-d). In DCX-positive cells of the DG from control animals, vertically oriented primary apical dendrites extended through the GCL and branched in the ML (a). On the other hand in Pb^{2+} -exposed animals, DCX-positive cells frequently had an irregular orientation of apical dendrites (see arrow heads in b and c), a “bushy” appearance or significant branching within the borders of GCL (see star in b). In addition, numerous apical dendrites often appeared dystrophic with a “spiral-like appearance (see arrows in c and d).

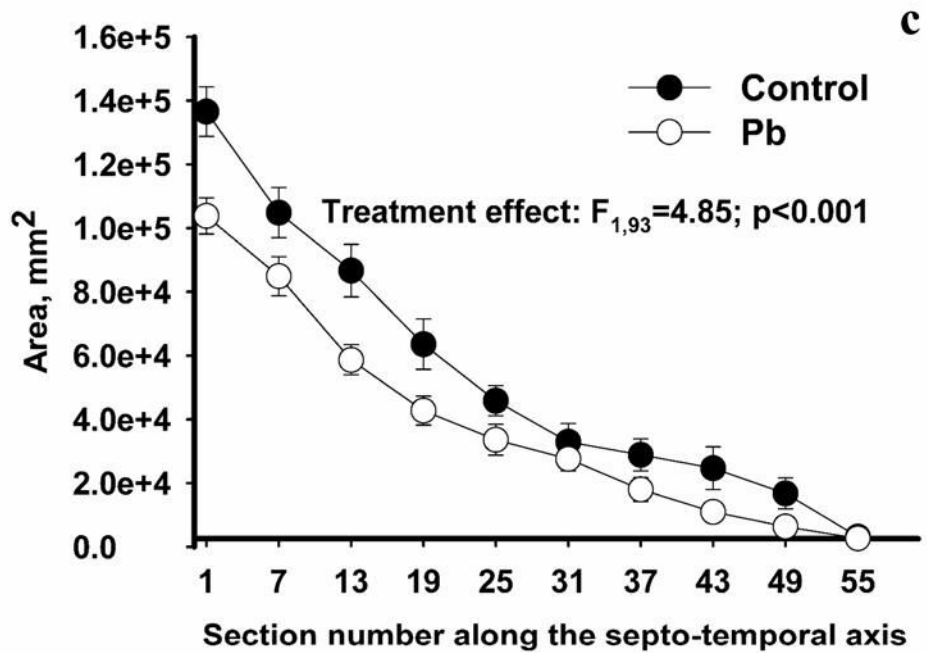
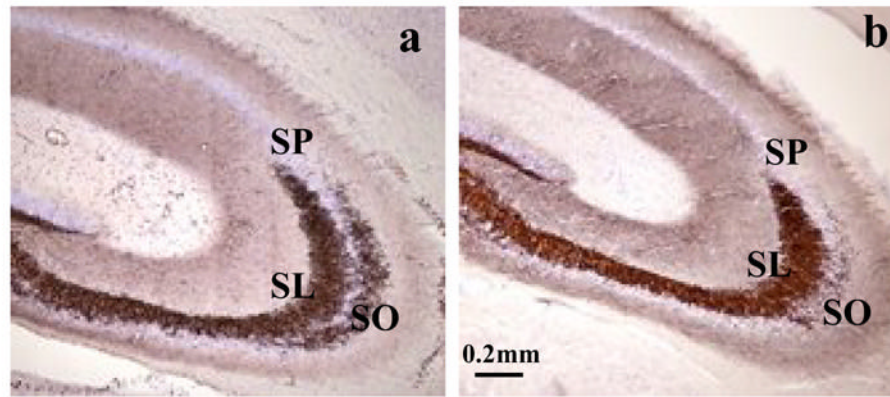


Figure 7.

Timm's and Nissl staining (a,b) in the hippocampus of control (a) and Pb²⁺-exposed rats (b). In control animals, Timm's stained mossy fibers were prominent in both the stratum lucidum (SL) and stratum oriens (SO) of the CA3 region (a). In Pb²⁺-exposed rats, reduced Timm's staining was detected in the CA3-SO. The stratum pyramidale (SP) is easily identified by Nissl staining. (b). The area of Timm's staining in the SO in the CA3 region was significantly diminished in Pb²⁺-exposed animals throughout the dorsal hippocampus (c). Each value is the mean \pm sem of n=6 different control animals and n=6 Pb²⁺-exposed animals.